Nonlinear Dynamics and Systems Theory, **21** (3) (2021) 229–237

Design and Analysis of Continuous Positive Airway Pressure Valve Using a 3D Printing and Computational Fluid Dynamic

S. Bentouati [1*], Mohamed Islem Soualhi [2], Abdellah Abdellah El-Hadj [1] and Hamid Yeklef [3]

[1] *Laboratory of Mechanics, Physics, Mathematical Modeling (LMP2M), University of Medea, Medea 26000, Algeria.*
[2] *Hospital of Ouargla, Intensive Care Unit, Algeria.*
[3] *Hospital Mohamed Boudiaf of Medea, Medical Equipment Maintenance Service, Algeria.*

Received: March 10, 2021; Revised: May 5, 2021

Abstract: The non-invasive ventilatory support in the Coronavirus (COVID-19) treatment uses also a mask as an interface between the medical device and the patient. The choice of this interface is one of the fundamental elements for the successful implementation of these techniques. The use of suitable equipment is also essential for their success, especially in continuous positive pressure with the mask (CPAP-continuous positive airway pressure) or during non-invasive two-level pressure ventilation. The criteria such as the ease of use and the required performance must be brought together in the medical equipment. With this aim, we will design a new version of the CPAP valve using the 3D printer, we used also the ANSYS software for the analysis and computation of the flow (CFD).

Keywords: *continuous positive airway pressure system; non-invasive ventilation; 3-dimentional printing; computational fluid dynamic.*

Mathematics Subject Classification (2010): 93A10, 93C95, 70K99.

* Corresponding author: mailto:bentouati.smain@gmail.com

1 Introduction

Ventilation is the only known treatment available for people with pulmonary failure caused by COVID-19. The resuscitation machines, that are at the disposal of hospitals, are complex and very expensive. Their availability is far from being close enough to meet the large number of patients received. For example, in our intensive care unit (in Medea, Algeria) we have around 7 machines that are currently functioning. So, given a large number of coronavirus patients that threaten to overwhelm our medical services, critically ill patients without ventilation treatment are at risk of losing their lives. To prevent this, we have designed CPAP (Continuous Positive Airway Pressure) valves, which help with artificial ventilation. The ventilatory assistance applied to patients in acute respiratory distress by NIV (non-invasive ventilation) is a very effective technique to avoid tracheal intubation [1, 2]. In this pandemic situation, the decathlon face mask (diving mask) is transformed to be used for medical purposes. We used it as the interface between the patient with coronavirus (Covid-19) and the valve we designed. It is therefore integrated in the kit shown in Figure 1. This valve is used to maintain continuous positive pressure throughout the respiratory cycle (during inspiration and expiration), which keeps the lungs open. NIV is an essential therapeutic mode in resuscitation and the evaluation of its practical use is very important and gives good results when controlling APE (Acute Pulmonary Edema) [3–5].

Figure 1: Yellow CPAP valve integrated in the kit, including, in particular, a pressure gauge (OHMEDA) and a ball flow meter which can vary from 0 to 30 l/min.

For the operation of the CPAP breathing valve, the quantity of oxygen arriving in an annular chamber is accelerated to the speed of sound as it passes through the microcannulas. This generates a high velocity flow in the center of the tube, which creates a zone of turbulence with the effect of separating the patient's respiratory volume (lungs and dead volume) from the outside air, without creating an airflow for the patient. It is the patient who will call for an air-oxygen mixture during inspiration. As we can see in Figure 2, the CPAP valve, which we manufactured in our laboratory using a 3D printer, is open on the atmospheric air side and works according to the Venturi effect. The turbulence zone acts as a virtual two-way valve that keeps the lungs under pressure during inspiration and creates a brake at expiration [6].

Finally, in this work, we will design a new version of the CPAP valve using the 3D

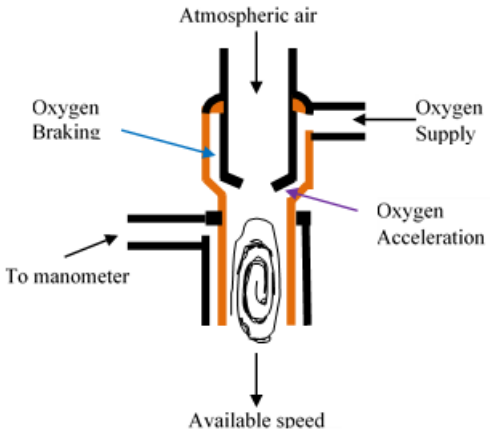

Figure 2: Diagram of the Boussignac CPAP System.

printer, the ANSYS software will be used for the analysis of the flow and the optimization of the parameters of this valve.

2 The CPAP Treatment Principle

For respiratory failure, the CPAP offers pupil oxygen levels, so it is attached to a flow of O_2, see Figure 3. In our case, O_2 is delivered to the patient by means of a diving mask, and the expiratory pressures are set above atmospheric pressure, therefore patients will breathe spontaneously during CPAP. The therapeutic use of CPAP is based on the delivery of high O_2 flow (FiO_2 from 35% to 90%) creating positive pressures of the respiratory tract which attract the open alveoli during the expiratory phase of the respiration allowing a longer time for exchanged gases. This results in physiological effects at high flow [7].

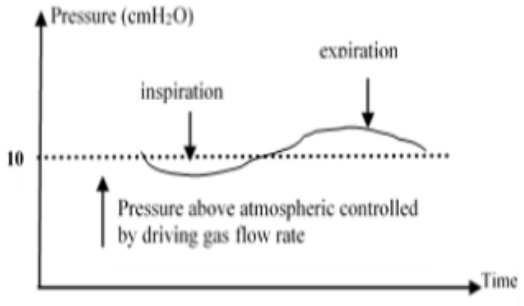

Figure 3: Profile of CPAP [7].

3 The CPAP Valve Design

CPAP is a ventilatory mode allowing to maintain in the airways a pressure higher than atmospheric pressure at the end of expiration [8, 9]. In spontaneous ventilation, the name is CPAP. In pre-hospital care, spontaneous positive pressure ventilation is indicated mainly in hemodynamic pulmonary edema (OAP) [10,11] when it is not possible to obtain a correct haematosis despite the FiO_2 of 100% (at least 70%) and when one wishes to avoid the tracheal intubation, and it is also indicated in patients with coronavirus (Covid-19). The non-invasive ventilation mode of this CPAP valve makes it possible to maintain airway permeability under positive pressure throughout the respiratory cycle, thus improving haematosis and decreasing respiratory work, this technique was first described and applied in 1930 for the treatment of OAP [12]. As you can see in Figure 4, the CPAP valve, which we made in our laboratory using a 3D printer, is open and works according to the Venturi effect [13,14]. Figure 5 shows a section view of the CPAP valve.

Figure 4: Representation of the CPAP valve that we manufactured (the left image: before assembly, the center image: complete assembly of the valve, the right image: comparison with the original valve).

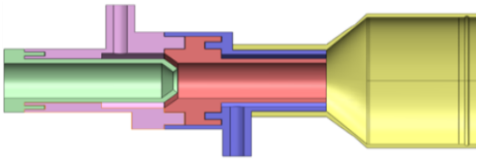

Figure 5: Detailed section view of the CPAP valve.

4 CFD Simulation

In this study, a finite volume method with ANSYS CFD is used to solve the set of equations system. We use one phase fluid flow instead of 3 phases (air, O_2, CO_2) in order to simplify the calculations. The fluid flow is considered to be turbulent. The standard $k-\varepsilon$ turbulence model has been widely used by researchers in many flow phenomena. The

$k-\varepsilon$ model is based on the Reynolds averaged Navier-Stokes (RANS) model. Supplementary terms of the Reynolds stresses are obtained, which require additional equations to solve them. This model uses two transport equations for turbulent kinetic energy (k) and its dissipation (ε) to solve for these terms. The governing equations for unsteady incompressible flow of a Newtonian fluid are given by [15]

$$\frac{\partial u_i}{\partial x_i} = 0, \tag{1}$$

$$\frac{\partial(\rho u_i u_j)}{\partial x_j} = \frac{\partial \rho}{\partial x_i} + \frac{\partial}{\partial x_j}[\mu(\frac{\partial u_i}{\partial x_j} + \frac{\partial u_j}{\partial x_i} - \frac{2}{3}\delta_i j \frac{\partial u_i}{\partial x_i})]. \tag{2}$$

The equations of the turbulent kinetic energy (k) and its dissipation (ε) are shown in Equations (3) and (4) as below:

$$\frac{\partial}{\partial x_j}(\rho k x_j) = \frac{\partial}{\partial x_j}[(\mu + \frac{\mu_t}{\sigma_k})\frac{\partial_k}{\partial x_j}] + G_k + G_b - \rho.\varepsilon, \tag{3}$$

$$\frac{\partial}{\partial x_j}(\rho \varepsilon u_i) = \frac{\partial}{\partial x_j}[(\mu + \frac{\mu_t}{\sigma_\varepsilon})\frac{\partial_\varepsilon}{\partial x_j}] + C_1\varepsilon\frac{\varepsilon}{k}(G_k + C_3\varepsilon G_b) - C_2\varepsilon\frac{\varepsilon^2}{k}\rho.\varepsilon. \tag{4}$$

The term G_k represents the generation of turbulence kinetic energy due to the mean of velocity gradients, which is given as $G_k = \mu_t S^2$ for the standard ($k\varepsilon$) model, where the modulus of the mean rate of strain tensor S is given as $S = 2S_{ij}^2$. S_{ij} is the symmetric deformation tensor equal to $\frac{1}{2}$ $(u_{ij} + u_{ji})$ The term of G_b is the generation of turbulence produced by buoyancy. On the other hand, $C_{1\varepsilon}$, $C_{2\varepsilon}$, $C_{\mu\varepsilon}$, σ_k and σ_ε are constants whose values are 1.44, 1.92, 0.09, 1, and 1.3, respectively, [16, 17].

4.1 Boundaries and boundary conditions

Figure 6 shows the mesh of the domain of interest and the different boundary conditions. There are two inlets. The turbulent intensity was set at 5% and the turbulent viscosity ratio was set as 10 (default values of fluent). The outlet was set as a pressure outlet, and the gauge pressure was set at 0 Pa, which means that the static pressure is equal to ambient pressure. In addition, the backflow turbulence intensity is 5% and the turbulent viscosity ratio is 10. The walls assumed no slip conditions and they were set to be stationary, as they do not move during the fluid flow.

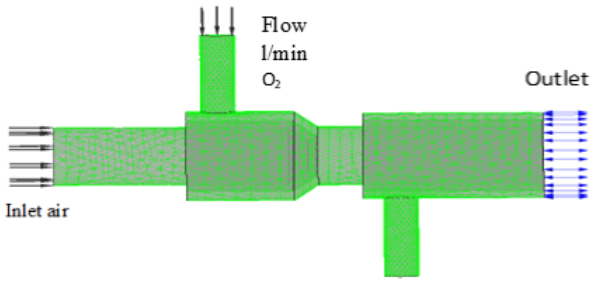

Figure 6: Mesh with boundary conditions.

4.2 Discretization schemes and algorithms

For this CFD problem, the finite volume method (FVM) scheme was implemented and utilised. A structural meshing technique is used to discretize the fluid domain. The set of the obtained RANS equations with boundary conditions are solved at each node of the mesh. The SIMPLEC algorithm (Semi-Implicit Method for Pressure Linked Equations-Consistent) is adopted in this study to calculate the pressures and velocities for the solution [18–21]. The solution is also affected by spatial discretization. For this purpose, the second order is used for pressure and momentum, and the first order is used for turbulent kinetic energy and its dissipation rate.

4.3 Numerical analysis results

Results of numerical simulations are presented in the following figures. Figure 7 shows the stream lines at the central plane at 4s.

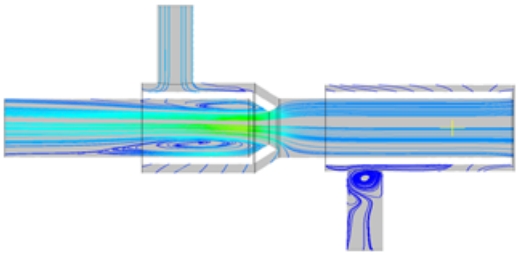

Figure 7: Streamlines at central plane at the time of 4s.

Figure 8 shows the simulation result of the pressure generated by the CPAP valve using the ANSYS CFD software. The pressure evolution during one cycle of breathing is presented here. A lot of physical parameters are introduced with a really very long computation time just to have this curve. So, we can see clearly the pressure which rises to around 15cmH_2O, then drops back to 5cmH_2O. However, in practice (Figure 9(b)), the pressure remains stable at around 7.5 cmH_2O during the inspiration stage.

5 Experimental Test of CPAP

As shown in Figure 9, in the resuscitation service in our region, we are testing our CPAP valve at the MEDEA hospital with pure oxygen via a ball flow meter that can vary from 0 to 20 l/min of brand (MedilineR), a manometer pressure (OHMEDA) indicating the pressure variation between inspiration and expiration to measure the positive expiratory pressure (PEEP).

To pass to expiration, the pressure of the gases exhaled by the patient must exceed the adjustment pressure of this valve indicated via the manometer. In fact, this pressure is proportional to the flow of oxygen. Hence, we have chosen to carry out our measurements by varying different O_2 levels in order to have a simple approach close to clinical values, Table 1 below indicates the O_2 flow rate required to achieve the desired PEEP pressures. We have compared, in Table 1, the practical results between the original Boussignac valve and our designed valve made in the laboratory using a 3D printer. First, we notice

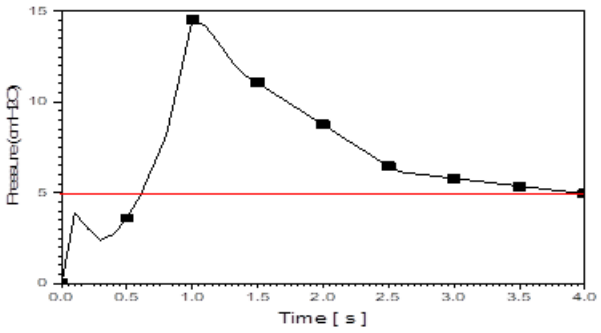

Figure 8: Pressure history at the outlet.

that the third column (our valve) reports good results. It is very important to note that the ICU doctors affirm that these results are very important at breathing difficulties.

Figure 9: CPAP valve integrated into the kit including a Decathlon mask, a flowmeter connected to the wall-mounted O_2 and a pressure gauge (the left image (a) with the original valve), (the center or the right image (b) and (c)) is indicating the variation in expiratory and aspiratory pressure).

O_2flow required(lit/min)	PEEP original valve(cmH_2O)	PEEP obtained(cmH_2O)
10	3	2
15	8	5.5
20	10	7.5

Table 1: Comparison of PEEP for experimental and numerical results for different O_2 flows.

6 Conclusion

In the present work, we have designed and fabricated a CPAP valve. In addition, a numerical study by the ANSYS software is done. The turbulent fluid flow is analysed in order to optimize the parameters provided by the valve. The tests that we have carried out experimentally in the MEDEA hospital, have given a satisfactory result. Finally, the valve we designed is easy to use in the intensive care unit with the advantage of providing proven respiratory support in VIN with a positive pressure. The PEEP is adjustable from 2 to 7.5 cmH_2O corresponding to the oxygen flow of 10 to 20l/min, respectively, according to the needs of patients with coronavirus (Covid-19).

Acknowledgment

The authors wish to thank the DGRSDT/MESRS, Algeria, for their financial support of this study.

References

[1] E. Mark, N. Stefano and B. Schonhofer. *Non-invasive Vebtilation and Weaning. Principal and Practice*. CRC Press, 2nd edition, 2018.

[2] G. Bellani, N. Patroniti, M. Greco, G. Foti and A. Pesenti. The use of helmets to deliver non-invasive continuous positive airway pressure in hypoxemic acute respiratory failure. *Minerva Anestesiol* **74** (2008) 651–656.

[3] F. Templier, F. Dolveck, M. Baer, F. Fernandez, M. Chauvin and D. Fletcher. Laboratory testing measurement of FIO_2 delivered by Boussignac CPAP system with an input of 100% oxygen. *Annales Franaises d'Anesthésie et de Réanimation* **22** (2003) 103–107.

[4] A. Mateos-Rodriguez and J. Ortega-Anselmi Francisco. Alternative CPAP methods for the treatment of secondary serious respiratory failure due to pneumonia by COVID-19. *Medicina Clinica* **156** (2) (2021) 55–60. https://doi.org/10.1016/j.medcli.2020.09.006.

[5] A. Paganoa, G. Portaa, et al. Non-invasive CPAP in mild and moderate ARDS secondary to SARSCoV2. *Respiratory Physiology and Neurobiology* (2020) Sep; 280: 103489. doi.org/10.1016/j.resp.2020.103489.

[6] B. Giacomo, F. Ester, S. Luigi, C. Nicolo and P. Antonio. An improved Boussignac device for the delivery of non-invasive CPAP: the SUPER-Boussignac. *Intensive Care Med.* **35** (2009) 1094–1099. DOI 10.1007/s00134-009-1403-x.

[7] G. Esmond and C. Mikelson. *Non-Invasive Respiratory Support Techniques, Oxygen Therapy, Non-Invasive Ventilation and CPAP*. Wiley-Blackwell Publ., 2009.

[8] F. Moritz, J. Benichou, et al. Boussignac continuous positive airway pressure device in the emergency care of acute cardiogenic pulmonary oedema: a randomized pilot study. *Eur. J. Emerg. Med.* **10** (3) (2003) 204–208.

[9] F. Templier, F. Dolveck, F. Baer, M. Chauvin and D. Fletcher. Boussignac continuous positive airway pressure system: pratical use in a prehospital medical care unit. *Eur. J. Emerg. Med.* **10** (2) (2003) 87–93.

[10] A.D. Bersten, A.W. Holt, A.E. Vedig and G.A. Skowronski. Treatment of severe cardiogenic pulmonary edema with continuous positive airway pressure delivered by face mask. *N. Engl. J. Med.* **325** (26) (1991) 1825–1830.

[11] M. Lin, Y.F. Yang, H.T. Chiang, M.S. Chang, B.N. Chiang and M.D. Cheitlin. Reappraisal of continuous positive airway pressure therapy in acute cardiogenic pulmonary edema: short-term results and long-term follow-up. *Chest* **107** (5) (1995) 1379–1386.

[12] E. L'Her. Non-invasive ventilation in acute respiratory distress. Réanimation et urgence médicales, CHU de la Cavale-Blanche, 29609 Brest cedex, France Article Original. 31-12-2004. ITBM-RBM **26** (2005) 41–50.

[13] D. Isabey, G. Boussignac and A. Harf. Effect of air entrainment on airway pressure during endotracheal gas injection. *Appl. Physiol.* **67** (1989) 771–779.

[14] B. Vallet, J. Leclerc, E. Plaisance and P. Goldstein. Intérêt de la ventilation non invasive au cours de l'insuffisance respiratoire aigüe, utilisation potentielle en médecine préhospitalière. In. Sfar, editor. Médecine d'urgence 1998. 40e congrès national d'anesthésie et de réanimation. Paris: Elsevier, 1998. P. 133–148.

[15] B.E. Launder and D.B. Spalding. *Lectures in Mathematical Models of Turbulence*. Academic Press, London, England. 1972.

[16] D. Khelfi, A. Abdellah El-Hadj and N. Ait-Messaoudene. Modelling of a 3D plasma thermal spraying and the effect of the particle injection angle. Revue des Energies Renouvelables CISM, 2008.

[17] D.C. Wilcox. *Turbulence Modeling for CFD*. La Canada, CA, DCW Industries, Inc., 1993.

[18] H.K. Versteeg and W. Malalasekera. An Introduction to Computational Fluid Dynamics – The Finite Volume Method. Addison-Wesley-Longman, 1995. ISBN: 978-0-582-21884-0.

[19] A.V. Artiukh, M.V. Sidorov and S.M. Lamtyugova. R-Functions and Nonlinear Galerkin Method for Solving the Nonlinear Stationary Problem of Flow around Body of Revolution. *Nonlinear Dynamics and Systems Theory* **21** (2) (2021) 138-149.

[20] A. Najafi and B. Raeisy. Boundary Stabilization of a Plate in Contact with a Fluid. *Nonlinear Dynamics and Systems Theory* **12** (2) (2012) 193-205.

[21] W. Parandyk, D. Lewandowski and J. Awrejcewicz. Mathematical Modeling of the Hydro-Mechanical Fluid Flow System on the Basis of the Human Circulatory System. *Nonlinear Dynamics and Systems Theory* **15** (1) (2015) 50-62.